P2.1 AMS 14th Symposium on Global Change and Climate Variations, 9-13 Feb. 2003, Long Beach, CA.

Long-term Variations in the 1000+ Year PCM Control Run

Aiguo Dai* , W.M. Washington, G.A. Meehl, A. Hu, T.W. Bettge, and W.G. Strand
National Center for Atmospheric Research (NCAR)$, Boulder, CO

Abstract

A 1200-year control run using the Parallel Climate Model (PCM), a fully coupled atmosphere-ocean-land-sea ice global climate model with no flux adjustments and relatively high resolution (~2.8° for the atmosphere and 2/3° for the oceans), is analyzed for unforced, long-term (decadal to multi-century) variations in surface temperature, precipitation, El Niño-Southern Oscillation (ENSO), the Arctic Oscillation (AO), and ocean circulations. The PCM produces relatively stable surface fields without flux adjustments, with a global surface cooling of –0.3°C per 1000 years and regional temperature trends comparable to those of flux-adjusted models. Global mean precipitation is highly correlated with global mean temperature, especially on decadal and longer time scales. Relatively rapid changes in global mean temperature and precipitation occurred a few times during the 1200-year integration. The PCM-simulated surface air temperature at the Greenland Ice Sheet Project Two (GISP2) site shows variation patterns comparable to those of GISP2 ice-core $\delta^{18}O$ record, although with much smaller variance. ENSO in this control run shows large variability at decadal to centennial time scales, with several periods (of decades) during which El Niños predominate. The PCM-simulated AO shows spatial and temporal patterns comparable to observed and exhibits little change during the integration. In this control run, the upper, clockwise overturning circulation in the Atlantic Ocean becomes increasingly shallow and weak while the bottom, anti-clockwise circulation gains depth and strength. The overturning changes are accompanied with an eastward shift of the central North Atlantic Drift Current. These ocean circulation changes are qualitatively similar to those in greenhouse gas-forced climate change simulations by the same model, although at a much slower pace. Nevertheless, this result suggests that interpretation of ocean circulation changes in greenhouse gas-forced model runs should be cautious and be put in the context of the changes in unforced control runs.

1. Introduction

Unforced, long-term (millennial) simulations of Earth's climate using fully coupled global numerical models consisting of the atmosphere, oceans, land, and sea ice have many important applications. For example, they can be used to quantify the internal variability in such models. This knowledge is essential for evaluating the significance of any model-projected climate changes under given forcing scenarios. Long-term climate simulations can also be used to study various modes of climate variability, such as the El Niño-Southern Oscillation (ENSO) and the North Atlantic Oscilltion (NAO) or the Arctic Oscillation (AO), on multi-century to millennial time scales, on which observations are rare. Such studies should help us understand some of the climate variations revealed by paleoclimate records, such as the abrupt climate changes (Alley et al. 2002).

It is, however, still a big challenging for current models to simulate the climate on centennial to millennial time scales without climate drifts (Stouffer et al. 2000). The unforced climate trends arise because current models still have deficiencies simulating many physical processes, such as the surface energy and momentum fluxes. Although very small, the errors accumulate in long-term simulations and result in noticeable trends in temperatures and precipitation. These unforced trends not only contaminate the model's internal variability, but also make the simulated climate unrealistic. In addition, fully coupled climate system models require a lot of computer resources for long-term runs, which makes them a daunting task. For example, the 1200-year simulation analyzed here took

* Corresponding author address: Aiguo Dai, NCAR/CGD, P.O. Box 3000, Boulder, CO 80307.

$ The National Center for Atmospheric Research is sponsored by the National Science Foundation.

about 456 days to complete on one of the fastest computers in the United States.

Here we report results from analyses of the 1200-year control run of the Parallel Climate Model (PCM) (Washington et al. 2000). The PCM is a fully coupled climate system model consisting of an atmospheric general circulation model (GCM), an ocean GCM, a land surface model, and a dynamic-thermodynamic sea-ice model. The PCM does not use flux adjustments and has a relatively high resolution (~2.8^{o} for the atmosphere and 2/3^{o} for the oceans). It produces a stable climate under current conditions that is comparable to observations (Washington et al. 2000; Dai et al. 2001a) and has near-observed El Niño amplitude (Meehl et al. 2001). The PCM has been used to simulate the 20th century climate (Dai et al. 2001b; Meehl et al. 2002) and the climate response to projected CO_2 and other emissions forcing in the next 1-2 centuries (Dai et al. 2001b,c). Compared with other millennial climate simulations (e.g., Stouffer et al. 2000), which were often run at reduced resolution and with flux adjustments, the PCM control run has the same resolution as in other production runs and has no flux adjustment.

2. Results

2.1 Global Temperature and Precipitation

Fig. 1 shows the globally averaged surface air temperature (solid line) and precipitation (dashed line) for model year 141-1199, with variations on shorter than 5 yr time scales being filtered out. First, the global mean temperature and precipitation are highly correlated, with correlation coefficient r=0.75 during 141-740 and 0.84 during 600-1199. This correlation is slightly weaker (r=0.65) for variations on shorter than 5 yr time scales, as precipitation exhibits larger variance on 2-5 yr time scales than temperature (Fig. 2). Second, both the temperature and precipitation are relatively stable from year 141 to ~450, then they decrease fairly rapidly and stay at a lower level for ~100 years. They recover slightly from year ~550 to 650, but never get back to the 141-450 level. Relatively rapid decreases occur again from year ~690 to 730. Thereafter, both the temperature and precipitation exhibit slow but steady decreases except for year 850-910 when they increase

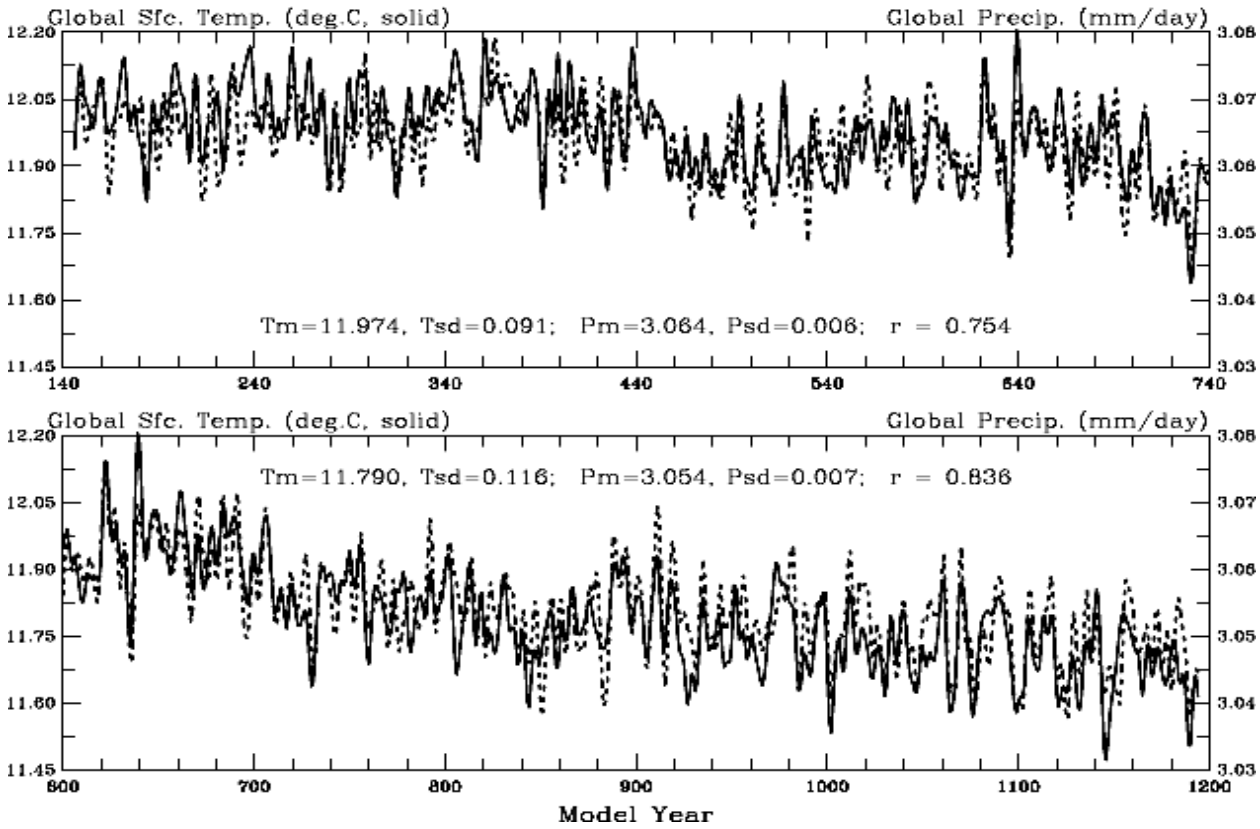

Fig. 1: Globally averaged surface (2 m) air temperature (*solid line*, ^{o}C on the left ordinate) and precipitation (*dashed line*, mm/day on the right ordinate) from model year 141 to 1199 of the PCM control run. Variations on shorter than 5 yr time scales were filtered out. Tm (Pm) and Tsd (Psd) are the mean and standard deviation of the time series within the corresponding panel. Also shown is the correlation coefficient (r) between the two curves.

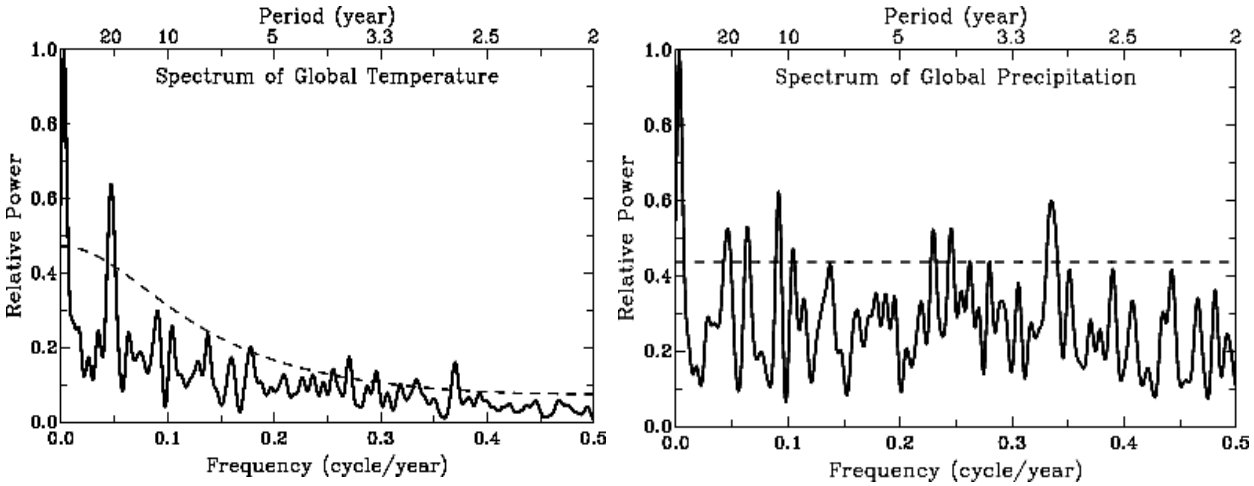

Fig. 2: Power spectra (normalized by the largest peak) of global-mean annual surface air temperature (*left*) and precipitation (*right*) from the PCM control run (year 141-1199) estimated using the fast Fourier transfer method. The dashed line is the 95% confidence level of a red (white) noise spectrum for temperature (precipitation).

slightly. Repeated runs around year 450 all show similar changes, suggesting that the relatively rapid changes occurred around year 450 (and 705) are likely to be real signal of the control run. The linear trend for the entire temperature series in Fig. 1 is about –0.3^{o}C per 1000 yr.

Fig. 2 shows the power spectra of global-mean annual surface air temperature and precipitation from the control run (year 141-1199). Statistically significant peaks for global temperature include those at 2.7, 3.7, 21 and 341 years. For global precipitation, the significant peaks are at 3.0, 4.1, 4.4, 11.0, 15.8, 21.8 and 341 years. As mentioned above, global mean precipitation has more relative power on 2-5 year time scales than global mean temperature.

Fig. 3 shows the geographical distribution of linear trends in surface air temperature during three different periods: year 141-440, 460-639, and 640-1199 of the control run. The magnitude of the regional trends over the entire period (141-1199) is comparable those of millennial simulations by other coupled models with flux adjustments (Stouffer et al. 200). During year 141-440, surface air temperature decreases (by 0.5-4.0^{o}C per 1000 yrs) over the Arctic region and most midlatitudes, while it increases (by 0.5-4.0^{o}C per 1000 yrs) over the Antarctica and southern midlatitudes, with negligible trends at low latitudes. The opposite trends compensate each other, resulting in small changes in global mean temperature during this period (Fig.1). It is possible that the PCM is still adjusting itself regionally during this period from the coupling of the ocean and atmospheric models. During year 460-639, both positive and negative trends exist at high latitudes of the two hemispheres, with large (3.0-4.5^{o}C per 1000 yrs) warming trends over Greenland. During year 640-1199, the trends become uniformly negative (i.e., cooling) over the globe, with larger magnitude at high latitudes (-0.5~-1.8^{o}C per 1000 yrs) than at low latitudes (-0.2~-0.4^{o}C per 1000 yrs). This uniform cooling results in a steady decline in global mean temperature during this period (Fig. 1). These results suggest that large regional trends can exist even if global mean temperature is stable and that regional adjustments in a coupled global model may take several centuries.

In order to compare the model-simulated temperature variability with that in paleoclimate records, in Fig. 4 we plotted the PCM-simulated surface air temperature time series at the Greenland Ice Sheet Project Two (GISP2) site (72^{o} 36' N, 38^{o} 30' W) together with the GISP2 oxygen isotope 18 (δ^{18}O) record of the last 1200 years (a proxy of paleo-air temperature over the region, see Cuffey et al.1995). The overall patterns of the two millennial time series are comparable. Both the time series have large decadal fluctuations and considerable centennial variations. The temperature standard deviation of the GISP2 record (1.3 K) is, however, about twice that (0.6 K) of the PCM-simulated time series. The latter is 2.8^{o} grid-box mean temperature, while the GISP2 record is from a single location. This may partly explain the larger variance in the GISP2 record. Both the (non-smoothed annual) time series have a red-noise type spectrum, with the PCM time

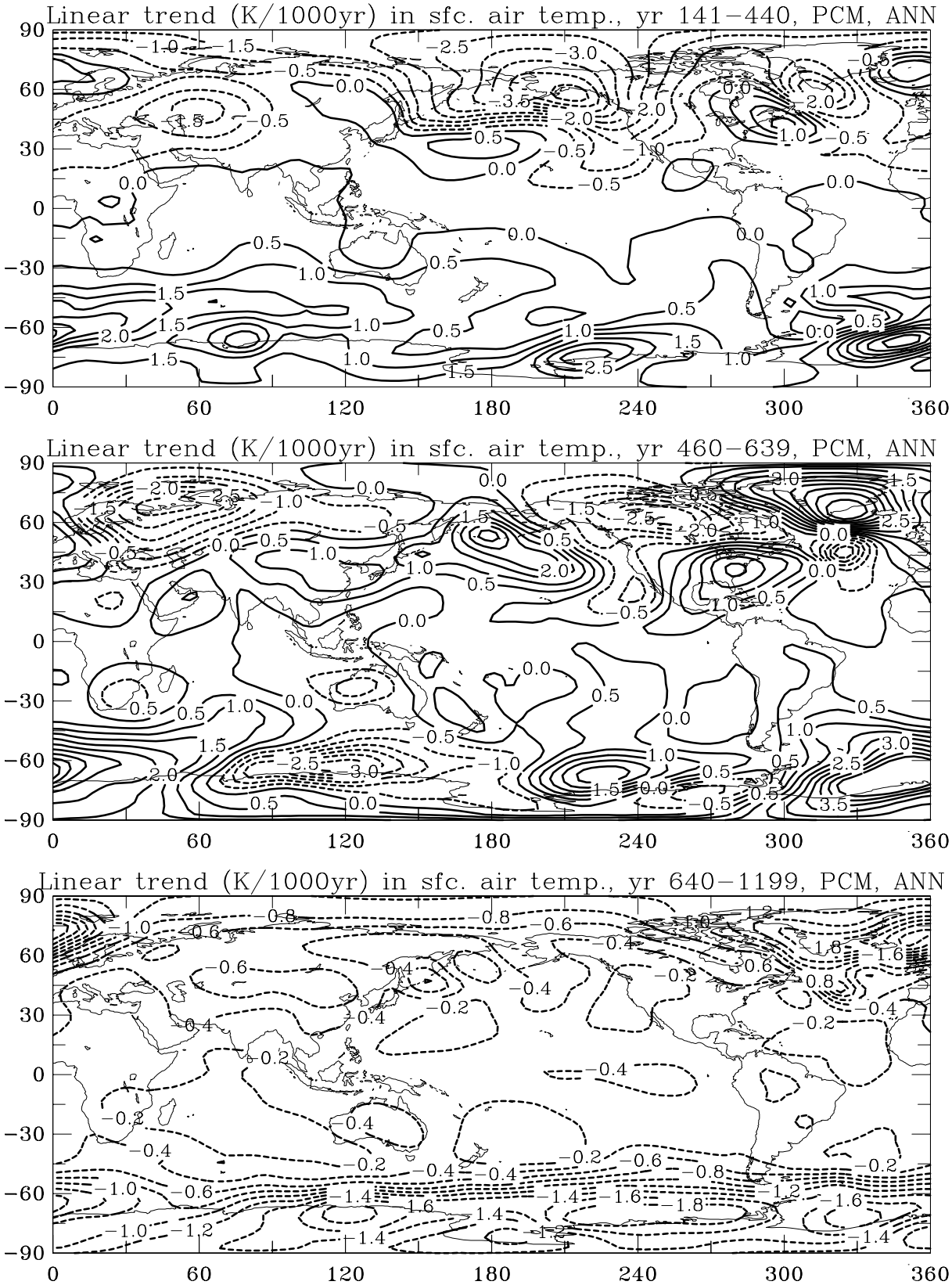

Fig. 3: Line trends (K/1000yr) of surface air temperature during three different periods of the PCM control run*: top:* year 141-440; *middle*: year 460-639; *bottom*: year 640-1199. Dashed lines indicate negative (cooling) trends.

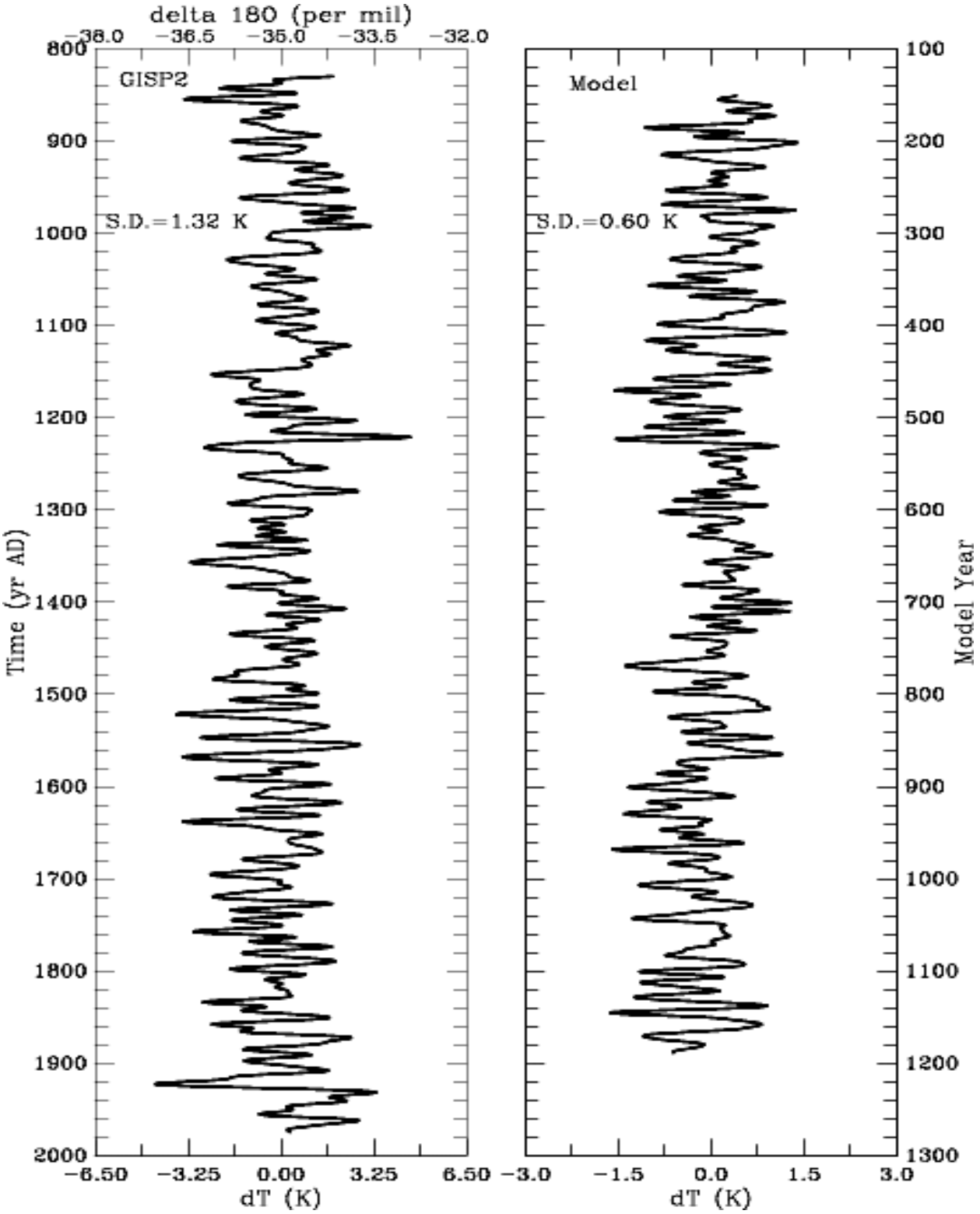

Fig. 4: *Left*: time series of the ice-core $\delta^{18}O$ record, a proxy of air temperature, from the GISP2 site in central Greenland (from Grootes et al. 1997). The temperature anomalies were estimated using $\delta^{18}O$ (per mil) = 0.46 T (K) + const (Cuffey et al.1995). *Right*: time series of surface air temperature anomalies (relative to the mean of the whole period) at the GISP2 site from the PCM control run. Variations on shorter than 10 yr time scales were filtered out in both plots.

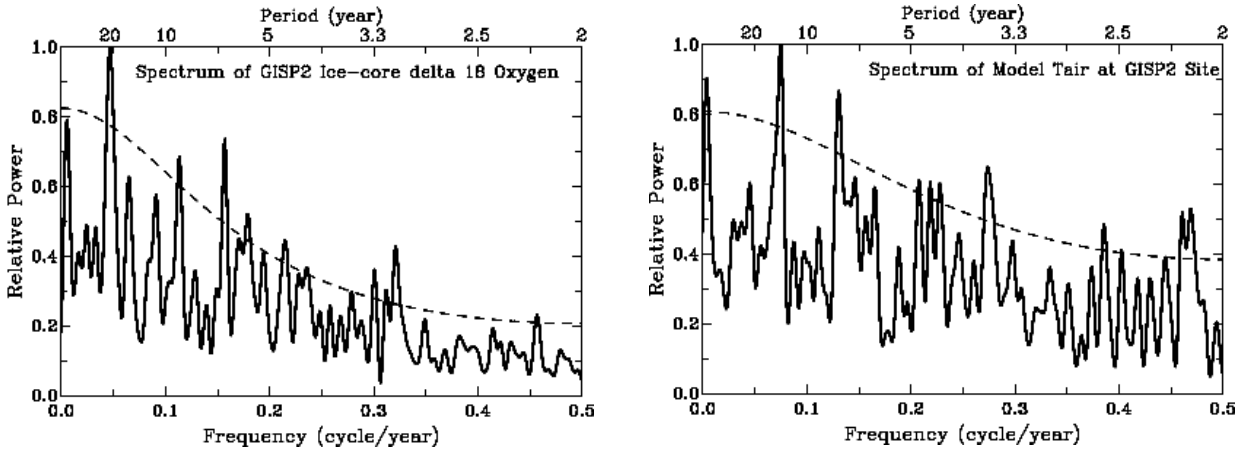

Fig. 5: Power spectra of the $\delta^{18}O$ (*left*) and PCM-simulated temperature (*right*) time series shown in Fig. 4 (before the filtering). The dashed line is the 95% confidence level of a red-noise spectrum.

series having more relative power on 2-3 year time scales (Fig. 5). The GISP2 record has a very strong peak around 21-yr period and significant peaks around 3.1, 6.4 and 8.8 years; while the PCM time series has significant peaks around 3.6, 7.6, 13.3 and 256 years (Fig. 5). These results suggest that the temperature time series from the PCM control run and the GISP2 ice-core $\delta^{18}O$ record exhibit comparable patterns of variability, although the ice-core record shows much larger variance than the PCM-simulated temperature (which is partly expected).

2 ENSO Activity

Fig. 6 shows the time series of normalized Niño 3 sea surface temperature (SST) anomalies from the PCM control run, together with color maps of relative power of variance of the SST time series as a function of the model year and time scales. It can be seen that the simulated Niño 3 SST is stable during the 1200-year simulation. Clearly, the frequency and magnitude of ENSO events exhibit large variations on decadal to centennial time scales. For example, ENSO is very weak during year 210-240 and 450-470, while it is very active during year 375-305, 385-410, 470-500, 1035-1055 and other periods. There are also periods during which warm events predominate (e.g., year 190-240, 745-795 and 1140-1195). This suggests that the predominance of El Niños since the middle 1970s (Trenberth and Hoar 1997) could partly result from natural variability.

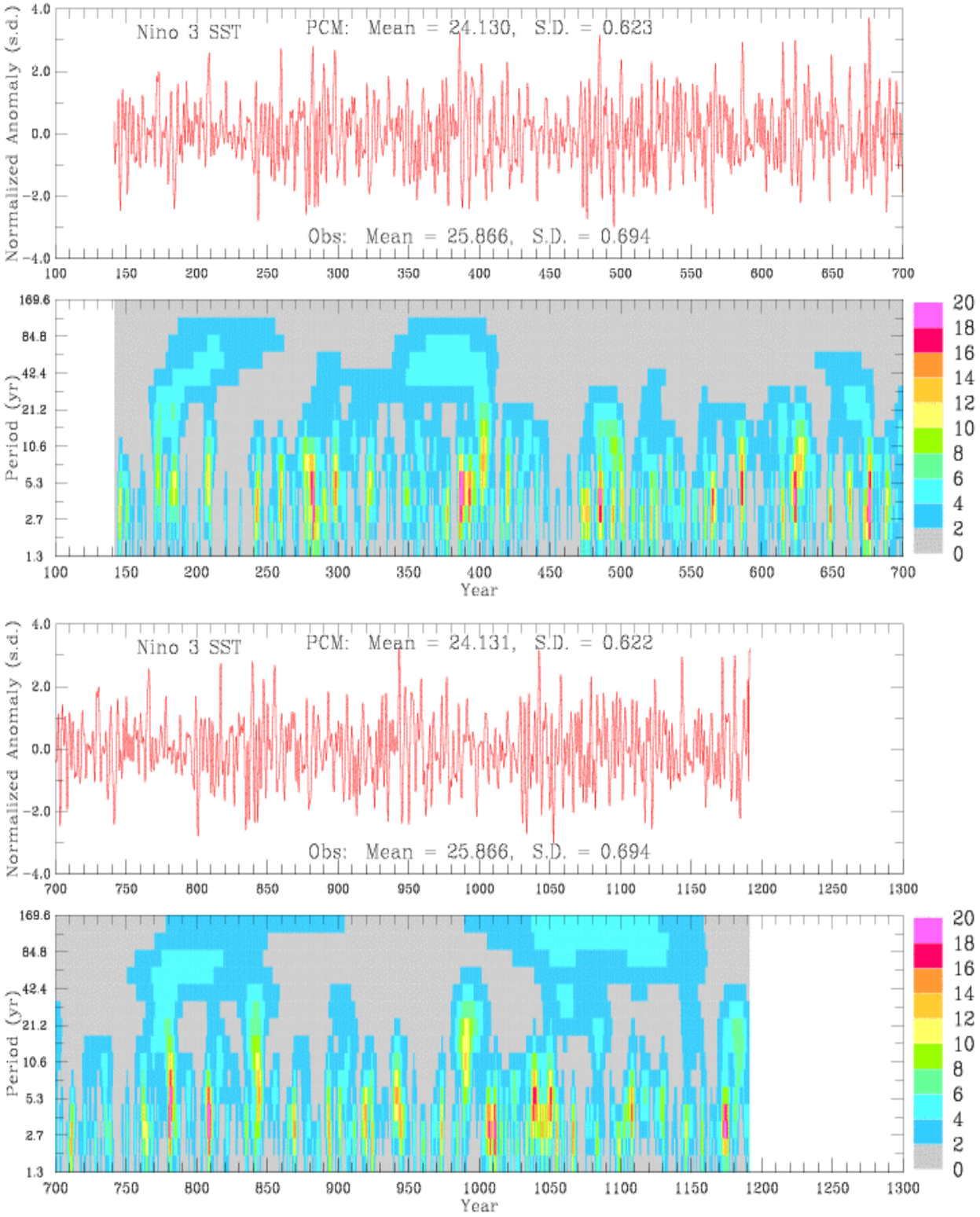

Fig. 6: Time series (red curve, normalized by standard deviation) and relative power of variance as a function of model year and time scales (color map, estimated using a wavelet analysis) of Niño 3 (5^{o}S-5^{o}N, 90^{o}W-150^{o}W) sea surface temperature from the PCM control run. Variations on shorter than 2-yr time scales were filtered out in the plotted time series. Also shown are the mean and standard deviation (S.D.) of the plotted time series and from observations of the last 30 years.

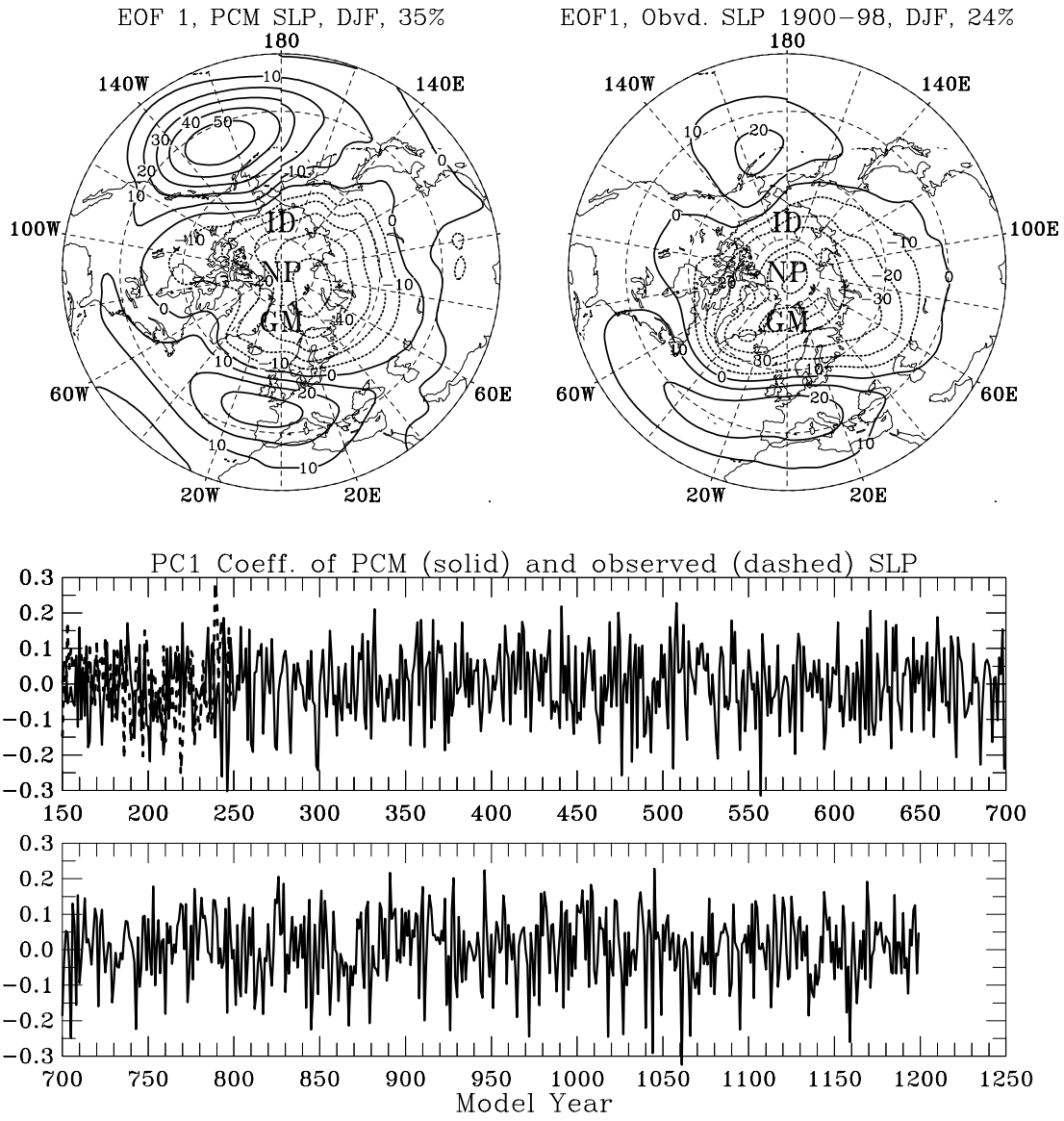

Fig. 7: The leading EOF of December-February (DJF) mean sea-level pressure north of 20°N from observations (*top right*, from Trenberth and Paolino 1980 and updates) and the PCM control run (*top left*). The lower panels show the time series of the principal component of the EOF for the model data, with that for the observations (for 1900-1998, dashed line) superposed with an arbitrary starting point. The explained percentage variance is also shown at the top.

2.3 Arctic Oscillation

Fig. 7 shows the leading empirical orthogonal function (EOF, or spatial pattern) and the time series of its temporal coefficient (or principal component) of the December-February (DJF) mean sea-level pressure for the domain north of 20°N from the PCM control run and the 20th century data (from Trenberth and Paolino 1980 and updates). The PCM captures the broad pattern of this so-called Arctic Oscillation (AO) or North Atlantic Oscillation (NAO), but the simulated mode has larger weighting over the North Pacific and accounts for a higher percentage of the total variance than the observations. The temporal coefficient of this mode exhibits no secular trends over the 1000+ year period, with the multi-year to decadal variations comparable to those of the 20th century.

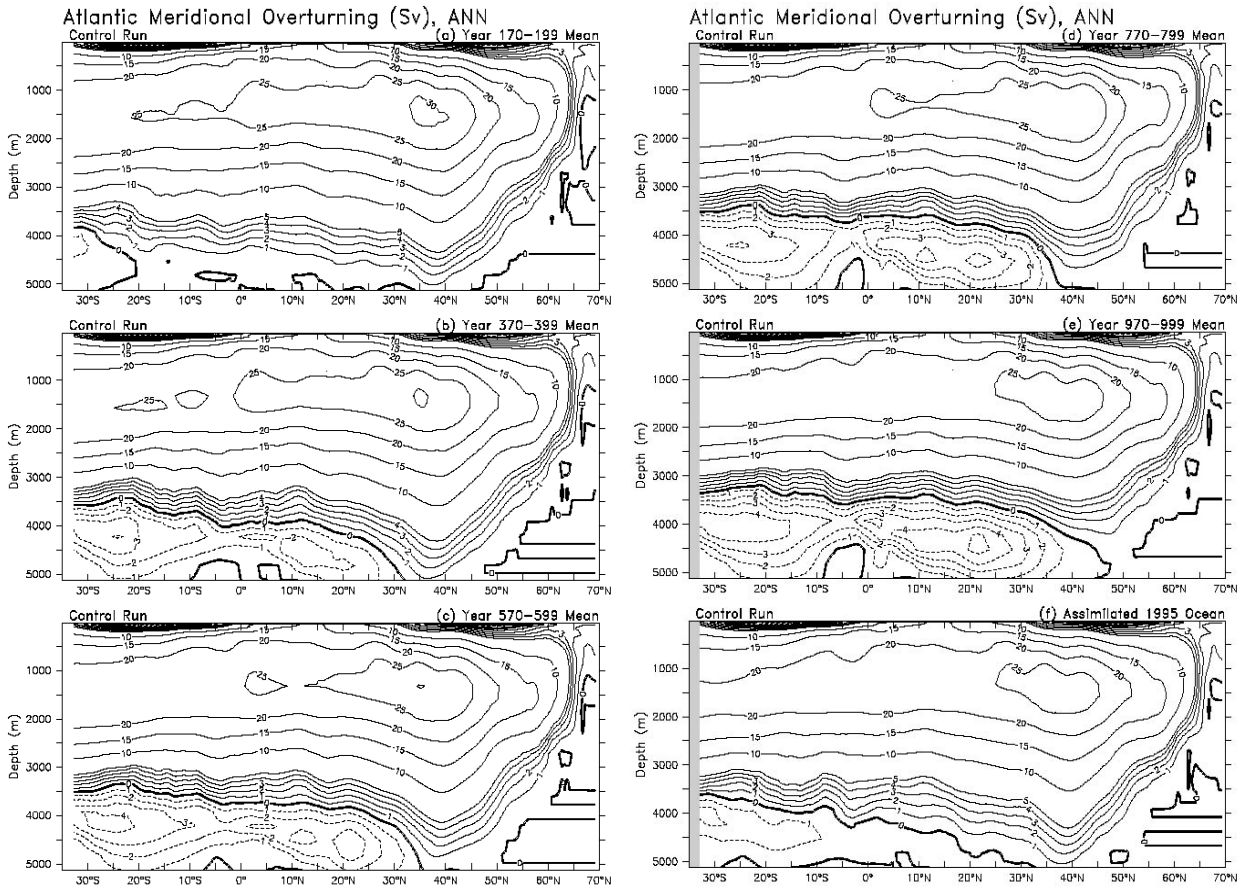

Fig. 8: Annual mean overturning streamfunction (*Sv*) of the Atlantic Ocean from the PCM control run for model year (a) 179-199, (b) 370-399, (c) 570-599, (d) 770-799, (e) 970-999, and (f) from data assimilation for 1995.

2.3 Ocean Circulation

Fig. 8 shows the annual mean overturning streamfunction of the Atlantic Ocean for various periods of the control run, together with an estimate for 1995 condition based on assimilated ocean data. The PCM-simulated overturning patterns during the first a few centuries are very close to the assimilated. Clearly, the upper, clockwise overturning cell becomes increasingly shallow and weak, while the bottom, anti-clockwise overturning cell gains depth and strength.

Fig. 9 shows the top 100m-averaged North Atlantic Ocean currents averaged over model year 350-369 and 970-999. The central North Atlantic Drift Current turns northeastward around 40^{o}W during the early centuries of the control run, but it makes this turn around 33^{o}W after about the sixth century. This eastward shift of the subtropical warm and saline water is accompanied by eastward expansion of arctic cold and fresh water, resulting in large surface cooling trends over the central midlatitude North Atlantic Ocean. These horizontal flow changes are likely to be linked to the overturning changes shown in Fig. 8, as the vertical and horizontal flows are closely coupled in the North Atlantic Ocean.

These ocean circulation changes are qualitatively similar to those seen in greenhouse gas-forced simulations by the PCM (Dai et al. 2001b), although at a much slower pace in the control run. These results suggest that there could be similar oceanic processes that lead to these changes in the forced and unforced simulations. Understanding of these oceanic processes will help us interpret the ocean circulation changes in greenhouse gas-forced climate change simulations.

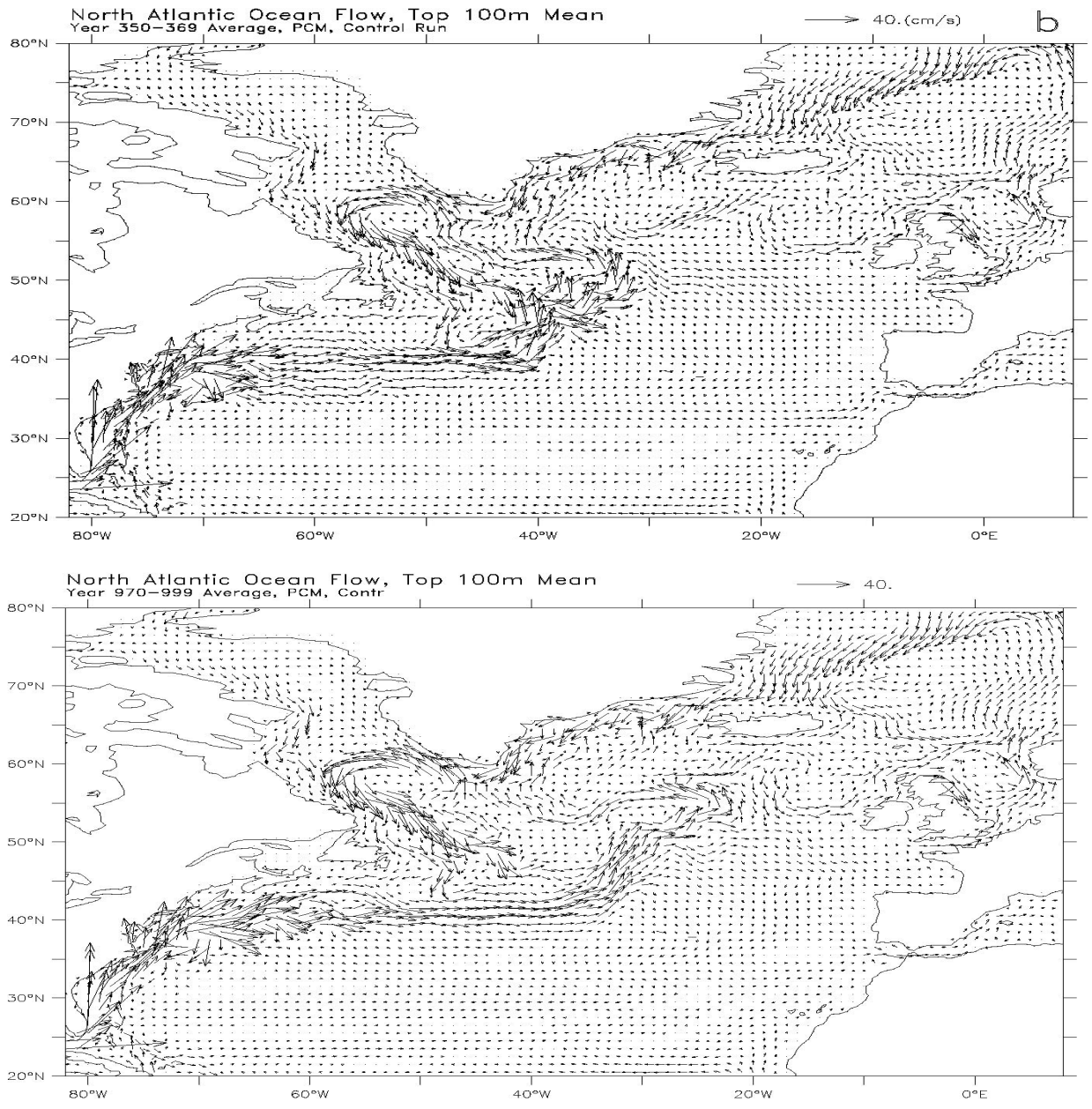

Fig. 9: Top 100m-averaged North Atlantic Ocean currents averaged over model year 350-369 (*top*) and 970-999 (*bottom*).

3. Summary

A 1200-year control run using the PCM was completed without using flux adjustments. The PCM control simulation, which was run at relatively high resolution compared with other millennial simulations, show a global cooling of –0.3°C per 1000 years and regional temperature trends (-0.2°C per 1000 yr in at low latitudes and up to –3.0°C per 1000 yr over the southern oceans) comparable to those of flux-adjusted models (Stouffer et al. 2000). Results show that substantial regional trends can exist even if the global mean temperature is stable. Global mean precipitation is highly correlated with global mean temperature in the control run, especially on decadal to centennial time

scales. Relatively rapid changes in global mean temperature and precipitation occurred a few times during the 1200-year integration. The PCM-simulated surface air temperature at the GISP2 site shows variation patterns comparable to those of GISP2 ice-core $\delta^{18}O$ record, although with much smaller variance. ENSO activity in the control run shows large variability at decadal to centennial time scales, with several periods (of decades) during which El Niños predominate. The PCM-simulated Arctic Oscillation shows spatial and temporal patterns comparable to observed and exhibits no secular trends in the long integration.

During the control run, the upper, clockwise overturning circulation in the Atlantic Ocean becomes increasingly shallow and weak, while the bottom, anti-clockwise circulation gains strength and depth. These overturning changes are accompanied with an eastward shift (of ~7^o longitude) of the central North Atlantic Drift Current., which allows cold and fresh arctic water to expand eastward, resulting in large surface cooling trends over the central North Atlantic Ocean. These ocean circulation changes are qualitatively similar to those in greenhouse gas-forced climate change simulations by the same model. This suggests that similar oceanic processes may lead to these ocean changes. This result suggests that interpretation of ocean circulation changes in CO_2-forced model runs should be cautious and be put in the context of ocean circulation changes in unforced model runs.

Acknowledgments: The PCM simulation was supported by the Department of Energy and the National Science Foundation.

Reference

Cuffey, K.M., G.D. Clow, R.B. Alley, M. Stuiver, E.D. Waddington, and R.W. Saltus, 1995: Large arctic temperature change at the Wisconsin-Holocene glacial transition. *Science*, **270**, 455-458.

Dai, A., G. A. Meehl, W. M. Washington, and T. M.L. Wigley, 2001a: Climate changes in the 21st century over the Asia-Pacific region simulated by the NCAR CSM and PCM. *Adv. Atmos. Sci.*, **18**, 639-658.

Dai, A., G.A. Meehl, W.M. Washington, T.M.L. Wigley, and J. A. Arblaster, 2001b: Ensemble simulation of twenty-first century climate changes: business as usual vs. CO2 stabilization, *Bull. Am. Met. Soc.*, **82,** 2377-2388

Dai, A., T.M.L. Wigley, G.A. Meehl, and W.M. Washington, 2001c: Effects of stabilizing atmospheric CO2 on global climate in the next two centuries. *Geophys. Res. Lett.*, **28**, 4511-4514.

Grootes, P.M. and M. Stuiver. 1997: Oxygen 18/16 variability in Greenland snow and ice with 10^3 to 10^5-year time resolution. *J. Geophys. Res.*, **102**, 26455-26470.

Meehl, G. A., P. R. Gent, J. M. Arblaster, B. Otto-Bliesner, E. C. Brady, and A. P. Craig, 2001: Factors that affect amplitude of El Ni\~{n}o in global coupled climate models, *Clim. Dyn.*, **17**, 515-526.

Meehl, G.A., W.M. Washington, T.M.L. Wigley, J.M. Arblaster, and A. Dai, 2002: Solar forcing and climate response in the 20th century. *J. Climate*, in press.

Stouffer, R.J.,G. Hegerl and S.Tett, 2000: A comparison of surface air temperature variability in three 1000-yr coupled ocean–atmosphere model integrations. *J. Climate*, **13**, 513–537.

Trenberth, K.E. and T.J. Hoar, 1997: El Niño and climate change. *Geophys. Res. Lett.,* **24**, 3057-3060.

Trenberth, K.E. and D.A. Paolino, 1980: The Northern Hemisphere sea level pressure data set: trends, errors and discontinuities. *Mon. Wea. Rev.*, **108**, 855-872.

Washington, W. M., J. W. Weatherly, G. A. Meehl, A. J. Semtner Jr., T. W. Bettge, A. P. Craig, W. G. Strand Jr, J. M. Arblaster, V. B. Wayland, R. James, and Y. Zhang, 2000: Parallel Climate Model (PCM) control and transient simulations. *Clim. Dyn.*, **16**, 755-774.